Sediment Dynamics at Kiri Dam (1982–2025): Bathymetry, Hypsographic Change, and Water-Supply Reliability

Gambo, Apagu Thliza[1*]; Olaniyan, O. S.[2]; Adegbola, A. A.[3]

[1,2,3]Department of Civil Engineering, Ladoke Akintola University of Technology, Ogbomosho, Nigeria

Corresponding Author: Gambo, Apagu Thliza[1*]

Abstract: This study presents the inaugural two-epoch comparison of Kiri Dam Reservoir in Nigeria, contrasting the 1982 design survey with a geodetically controlled hydrographic resurvey conducted in 2025. The methodologies employed adhered to IHO S-44 (2020) standards, including Trimble RTK-GNSS control, ADCP depth soundings, crossline calibration, uncertainty propagation, TIN and raster surface generation, and hypsographic volume integration. At NTWL (170.5 meters above mean sea level), live storage has decreased from 615 million cubic meters to 344.15 million cubic meters (a reduction of 44.04%), and the surface area has declined from 106.36 to 67.02 square kilometres (a decrease of 37%). These losses are concentrated in the 161–167 metre benches, as confirmed by PSD analyses of silty clay and geochemical fingerprinting indicating organic-rich fines. Regression analyses reveal strong linear relationships for elevation–capacity, with R^2 values of 0.996 in 1982 and 0.992 in 2025. The results suggest diminished irrigation reliability and limited flood buffering capacity, emphasizing the need for targeted sediment management and periodic resurveying.

Keywords: *ADCP, Bathymetry, Elevation–Capacity, Geochemistry, Hypsography, IHO S 44, Kiri Dam, Nigeria, PSD, Reservoir Sedimentation.*

How to Cite: Gambo, Apagu Thliza; Olaniyan, O. S.; Adegbola, A. A. (2025) Sediment Dynamics at Kiri Dam (1982–2025): Bathymetry, Hypsographic Change, and Water-Supply Reliability. *International Journal of Innovative Science and Research Technology,* 10 (9), 355-368. https://doi.org/10.38124/ijisrt/25sep171

I. INTRODUCTION

Reservoir sedimentation alters the elevation–area–capacity curve, affecting storage capacity for water supply, flood control, and environmental releases. This deterioration results from catchment erosion and hydraulic sorting: coarse particles deposit at delta fronts, while fine sediments like silts and clays settle in lower-energy zones over time (Kondolf *et al*., 2014; Morris & Fan, 1998). Research links capacity loss in tropical and semi-arid areas to land-use change, rainfall, and morphometry (Li *et al.,* 2020; Domínguez-Gálvez & Álvarez-Álvarez, 2025; Punuf *et al*., 2025). Repeat bathymetry provides a standard method to identify hypsographic changes and distinguish true geomorphic shifts from measurement errors (IHO, 2022; USACE, 2013). Without geodetically controlled resurveys, rule-curve calibration and sediment management rely on assumptions instead of empirical data.

In West Africa's Sudano–Sahel, seasonal hydrological changes, bank erodibility, and fragile soils increase sediment transfer from hillslopes to channels and reservoirs (Li *et al*., 2020). Regional studies show morphodynamical changes and

siltation in large reservoirs; however, few have two-epoch, standards-compliant bathymetric comparisons that measure deformation of the elevation–area–capacity curve and identify the most affected elevation bands (Kondolf *et al*., 2014). This gap is critical: operational and maintenance decisions—like dredging, sluicing, drought, and flood planning—rely on understanding shoaling patterns and their impact on intakes, conveyance, and spillways (Morris & Fan, 1998; USACE, 2013). A rigorous reassessment must ensure (i) geodetic accuracy, (ii) address uncertainty, and (iii) align with historical records for comparable analysis (IHO, 2022).

This study establishes a dual-epoch framework for Kiri Dam, Nigeria, adhering to IHO S-44 recommendations. It uses RTK-GNSS/DGPS control with high-density hydroacoustic depth acquisition (ADCP), supported by sound-speed casts, patch testing, bar checks, residual targets, and uncertainty analysis to generate georeferenced point clouds for change detection (IHO, 2022; USACE, 2013). Cleaned soundings are triangulated into a TIN, rasterized with shoreline breaklines, and integrated via the trapezoidal rule to derive elevation-area and capacity data aligned with standard practices (USBR, 1985). The morphometric analysis

combines sediment particle-size distributions (PSD) and geochemical indicators—pH, TOC, TN, phosphorus, trace metals—using APHA methods to test hypotheses about trapping fine, organic-rich fractions on mid-reservoir benches (APHA, 2017; Li *et al.,* 2020). The result is an evidence-based, reproducible framework that identifies elevation bands with high-capacity recovery potential and risk mitigation, along with proper archiving and metadata.

The study aims to: (i) create a geodetically referenced bathymetric surface and an updated elevation–area–capacity dataset for Kiri Dam using IHO procedures; (ii) analyse sedimentation patterns by elevation to identify zones of deposition; and (iii) interpret PSD and geochemical data with morphometric changes to assess sediment-transport controls and water-supply risks (Kondolf *et al.*, 2014; APHA, 2017; IHO, 2022). This framework avoids assumptions; detailed results are in later sections.

II. METHODOLOGY

➢ Study Area
Kiri Dam (Gongola River, Upper Benue Basin) supplies irrigation and regional water resources. The methodologies adhere to IHO S-44 (2020) standards. All coordinate data are referenced to WGS 1984 UTM Zones 32N/33N.

➢ Reconnaissance and Access Controls
Reconnaissance mapped submerged trees, Typha, gill nets, and hippopotamus colonies. Navigation routes, launch/egress points, and instrument security were established. Only factors affecting transect design, safety, and data density were retained in technical logs.

➢ Geodetic Control (Horizontal and Vertical)
A temporary GNSS base station (E 172348.341 m; N 1071421.496 m; z 173.442 m) was positioned at the dam axis. Ten permanent beacons, approximately 2.5 km apart, linked the survey to dam benchmarks. Static and rapid-static solutions achieved root mean square errors (RMSE) of less than or equal to 0.03 m in the horizontal plane and less than or equal to 0.05 m in the vertical direction. Water level measurements obtained from staff gauges on the crest were used for water level reductions; daily loop closures were employed to monitor and control drift.

➢ Hydroacoustic Acquisition and Navigation
Primary depths were assessed using a boat-mounted ADCP operating within the frequency range of 600–1200 kHz, utilising cells of 0.25–0.50 meters, with pings conducted at a rate of at least 1 Hz. A legacy single-beam system, comparable to Garmin class equipment, was employed for validation purposes. Transects were designed to be quasi-orthogonal, with spacing of 50–75 meters near steep banks and 100–150 meters in the mid-reservoir region; at least 10% of the lines constituted crosslines for independent verification. In hazard zones, vessel speed was confined to the range of 1.5–2.5 meters per second.

➢ Calibration, QA/QC, and Uncertainty Propagation

- Sound speed: morning/afternoon CTD casts; Del Grosso/Mackenzie corrections.
- Patch tests: latency/roll/pitch/yaw at start and after mount changes.
- Bar checks: daily vertical scale verification for single-beam.
- Editing: Hampel filtering; amplitude/SNR thresholds; cull |roll| or |pitch| > 10°.
- Crossline residuals: median absolute vertical ≤ 0.12 m.
- Uncertainty model: $u_z = \sqrt{u_{GNSS}^2 + u_{SS}^2 + u_{att}^2 + u_{edit}^2}$ rasterized to support error bars in summary plots.

➢ Surface Generation and Volumetrics
Soundings were triangulated to TIN (ArcGIS 10.1) and rasterized at 5–10 m resolution using shoreline breaklines. Volumes used trapezoidal integration:

$$V = \sum_{i=1}^{n-1} \frac{(A_i = A_{i+1})}{2} \times (h_{i+1} - h_i) \qquad (2.1)$$

➢ Sediment Sampling, PSD, and Geochemistry
Samples of sediments from inflow, mid-reservoir, outflow, and from both the left and right banks were subjected to comprehensive analysis. Particle size distribution (PSD) was ascertained utilising a hydrometer. The geochemical parameters evaluated included pH, Total Organic Carbon (TOC), Total Nitrogen (TN), Phosphorus, Lead (Pb), Copper (Cu), Zinc (Zn), Total Polycyclic Aromatic Hydrocarbons (ΣPAHs), Total Polychlorinated Biphenyls (ΣPCBs), and Specific Gravity. All analytical procedures strictly conformed to the standards delineated in the APHA (2017) protocol.

➢ Data Management and Reproducibility
All raw and processed artefacts, including GNSS, sonar, CTD, logs, QA/QC data, TINs, and rasters, are archived with ISO 19115/19157 metadata. Figures and tables can be reproduced through scripted GIS and analysis notebooks.

III. RESULTS AND DISCUSSION

This section summarizes bathymetric reductions, revised E–A–C relations, and banded capacity/area losses, followed by an evaluation of areal distribution, PSD, and geochemistry to diagnose morphodynamic controls. The findings are presented alongside stated uncertainties and conclude with a synthesis of operationally relevant elevation bands.

➢ Bathymetric Surface and Hypsography (2025)
The 2025 survey provided a refined, geodetically referenced point cloud and a processed bathymetric surface for volumetric and morphometric analyses (Figures 1–2). ADCP depths were calibrated to water levels, integrated with GNSS data, triangulated into a TIN, and rasterized at 5–10 meters resolution in ArcGIS 10.1; volumetric calculations used band-wise trapezoidal integration (Eq. 2.1). These methods are standard in reservoir sedimentation studies,

especially when distinguishing planform change and hypsographic deformation from artefacts (e.g., Domínguez-Gálvez & Álvarez-Álvarez, 2025).

The processing procedures and uncertainty management follow IHO S-44 (IHO, 2020) standards. Surfaces and contours provide the empirical basis for later elevation–area–capacity (E–A–C) diagnostics.
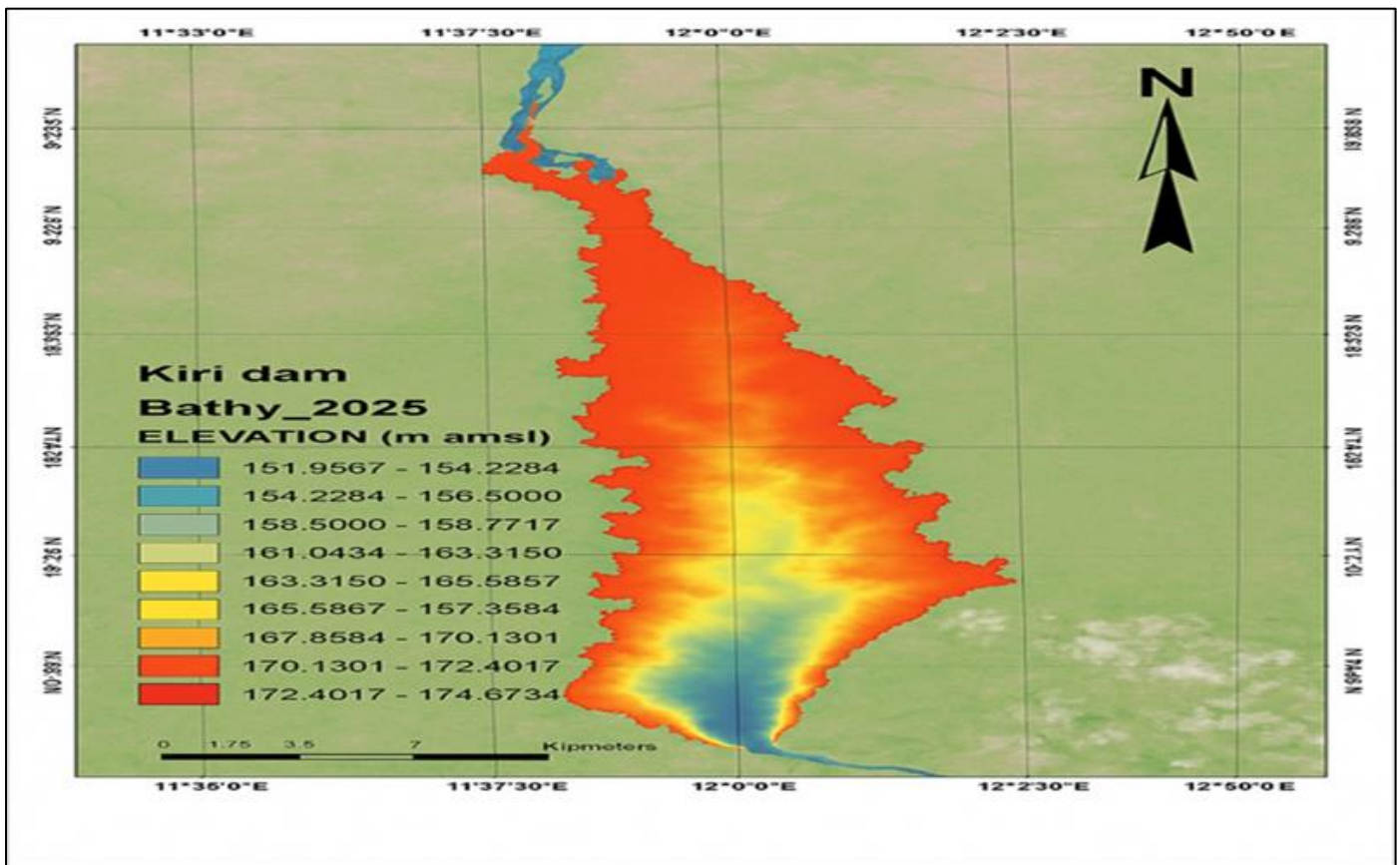

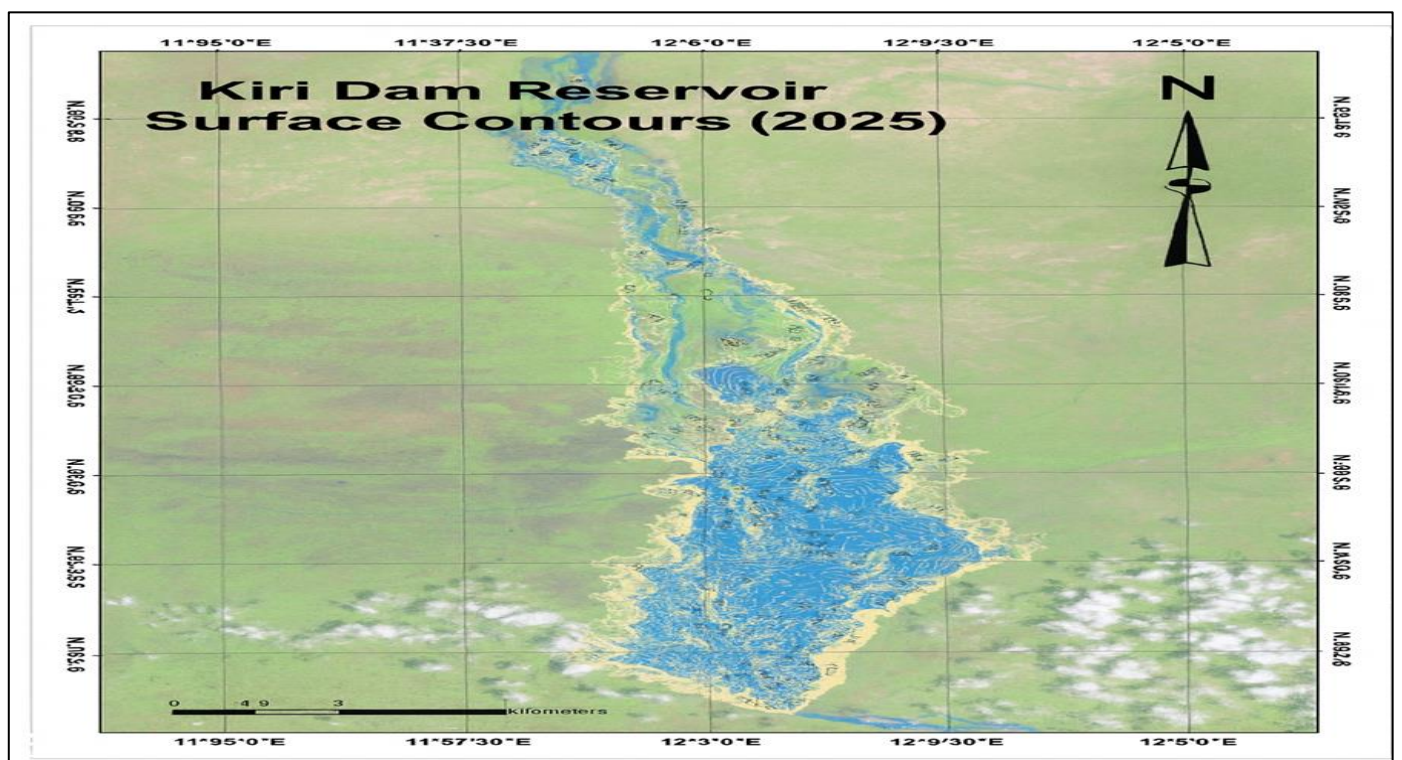Fig 1 Bathymetric Survey Map of Kiri Reservoir Bed Topography (2025)

Fig 2 Kiri Dam Reservoir Surface Contours (2025)

➢ *Revised Elevation–Area–Capacity Relationship (2025)*

The revised E–A–C dataset ranges from 151.96 to 174.67 meters above sea level. At NTWL = 170.5 meters, storage capacity is 344.15 MCM over 67.02 km² (see Table 1). The curve steepens between 161 to 167 meters (see Figure 3). Cumulative capacity was calculated from raster data using Equation 1. The curvature indicates preferential infilling in reservoirs in semi-arid and tropical areas (Domínguez-Gálvez & Álvarez-Álvarez, 2025; Punuf *et al.*, 2025). Capacity was computed using hypsographic methods per IHO (2020). The 2025 curve shows compressed live storage, guiding monitoring at mid-bench levels.

Table 1 Revised Kiri Reservoir Area–Elevation–Capacity (2025)

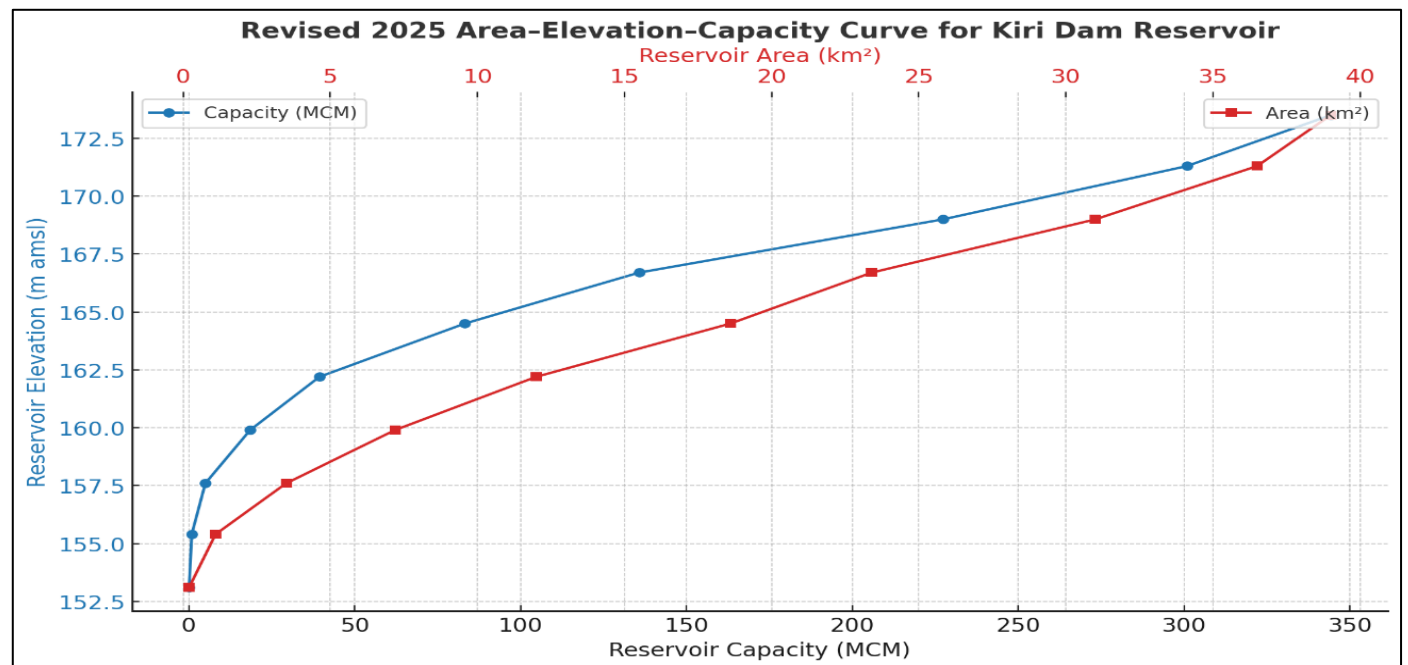| Elevation (m amsl)	Area (km²)	Capacity (MCM)
151.96–154.23	0.2	0.1
154.23–156.50	1.1	0.9
156.50–158.77	3.5	5
158.77–161.04	7.2	18.5
161.04–163.32	12	39.4
163.32–165.59	18.6	83.2
165.59–167.86	23.4	135.7
167.86–170.13	31	227.3
170.13–172.40	36.5	300.8
172.40–174.67	39	344.15

Fig 3 Revised 2025 Area–Elevation–Capacity Curve for Kiri Dam Reservoir

➢ *Capacity and Surface-Area Losses Relative to 1982*

Compared to the 1982 NTWL design (615 MCM; 106.36 km²), 2025 data shows a capacity reduction of −270.83 MCM (−44.04%) and surface area decrease by −39.34 km² (−37%), as detailed in Table 2. Over 60% of capacity loss occurs below 167 meters, shown in Figure 4. These losses were identified through band-by-band comparison of 1982 and 2025 E–A–C values. Mid-reservoir attrition aligns with global patterns where hydraulic sorting traps silt and clay on interior shelves (Morris & Fan, 2019; Li *et al.*, 2020). Cross-epoch comparisons used vertical control measures and included IHO (2020) uncertainty. Isolated forebay interventions are inadequate; elevation-focused strategies are needed to restore storage capacity.

Table 2 Capacity and Area Losses Between 1982 (Design) and 2025 (Survey)

Elevation (m amsl)	Capacity 1982 (MCM)	Capacity 2025 (MCM)	Loss (MCM)	% Loss	Area 1982 (km²)	Area 2025 (km²)	Loss (km²)	% Loss
151.96–154.23	0.05	0.1	−0.05	0.00	0.05	0.2	−0.15	0.00
154.23–156.50	1.00	0.90	0.10	10.00	1.30	1.10	0.20	15.40
156.50–158.77	7.00	5.00	2.00	28.60	5.10	3.50	1.60	31.40
158.77–161.04	25.30	18.50	6.80	26.90	10.20	7.20	3.00	29.40
161.04–163.32	55.00	39.40	15.60	28.40	17.10	12.00	5.10	29.80

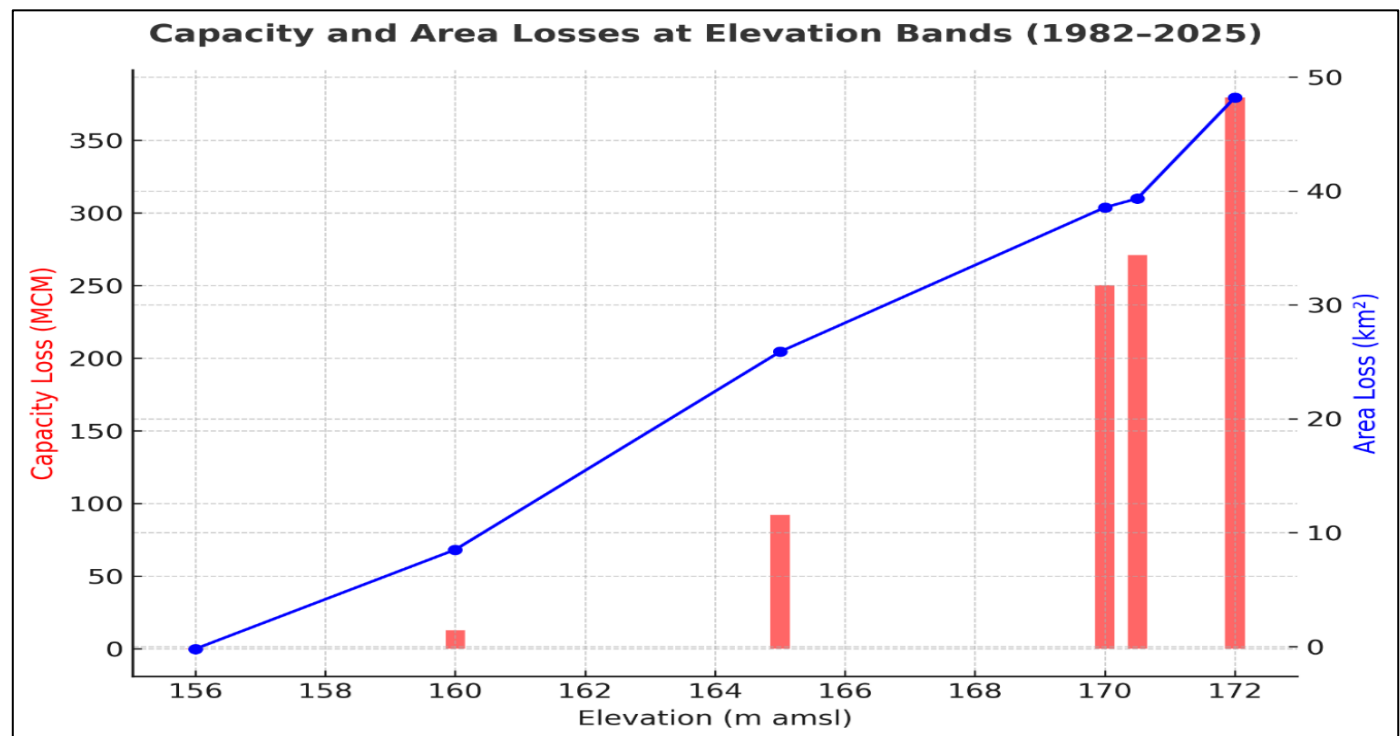| 163.32–165.59 | 110.00 | 83.20 | 26.80 | 24.40 | 25.30 | 18.60 | 6.70 | 26.50 |
165.59–167.86	160.00	135.70	24.30	15.20	30.00	23.40	6.60	22.00
167.86–170.13	220.00	227.30	−7.30	0.00	38.00	31.00	7.00	18.40
170.13–172.40	340.00	300.80	39.20	11.50	49.00	36.50	12.50	25.50
172.40–174.67	615.00	344.15	270.85	44.04	106.36	67.02	39.34	37

Fig 4 Capacity and Area Losses at Elevation Bands (1982–2025)

➤ *Areal Distribution of Elevation Bands and Correlation Structure*

The classification indicates that over 54% of the water spread occurs at an elevation of ≥170 meters above mean sea level (delta front/plain; Table 3). Regression analyses substantiate strong linear relationships across different epochs (1982: $R^2 = 0.996$; 2025: $R^2 = 0.992$), and a significant correlation exists between area and capacity within the range of 161–167 metres ($r=0.88$, $p<0.01$; Fig. 3.5a–b). The band areas utilized were derived from the 2025 raster dataset; ordinary least squares (OLS) regressions were employed to evaluate linearity and leverage.

Elevation-band leverage is common in scenarios where minor vertical aggradation across extensive benches leads to notable volume penalties (*Li et al.,* 2020). Statistical summaries serve as a supplement to hydrographic quality assurance and quality control (QA/QC) by quantifying the spatial coherence of changes (International Hydrographic Organisation, 2020). The predominance of shallow depositional processes diminishes hydraulic efficiency and accentuates the influence of centimetre-scale aggradation on usable storage capacity.

Table 3 Areal Distribution of 2025 Bathymetric Elevation Bands

| Elevation Range (m a.m.s.l.)	Area (km²)	% of Total	Functional Interpretation
151.96–154.23	0.2	0.3	Deep thalweg
154.23–156.50	1.1	1.6	Persistent deep pool
156.50–158.77	3.5	5.2	Transition zone
158.77–161.04	7.2	10.7	Mid-reservoir benches
161.04–163.32	12	17.9	Bench/delta transition
163.32–165.59	18.6	27.8	Mid-reservoir shoals
165.59–167.86	23.4	35	Shoaling reaches
167.86–170.13	31	46.2	Shallow depositional bench
170.13–172.40	36.5	54.5	Delta front
172.40–174.67	39	58.2	Delta plain/upper shoals
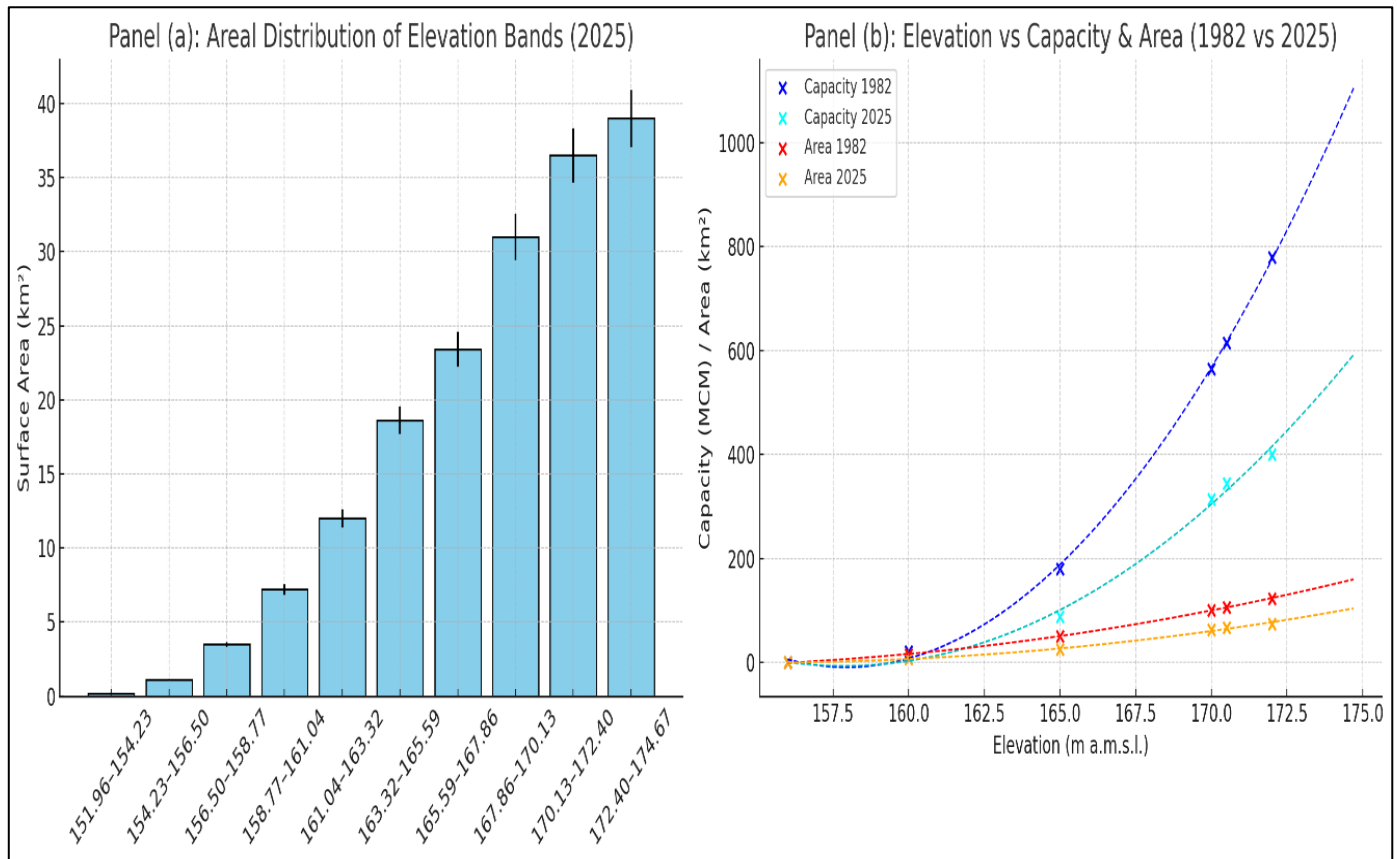
Fig 5 Areal Distribution and Statistical Correlation of Elevation Bands (2025):

- *Panel A: Areal distribution of 2025 elevation bands (km² vs elevation); (b) Panel B: Regression plots of elevation–capacity and elevation–area (1982 vs 2025) showing strong positive correlations (R² = 0.996; R² = 0.992).*

➢ *Integrated Operational Comparison at Key Levels*

Control elevations at 156–172 m a.m.s.l. reveal a non-linear escalation of storage and area losses, culminating at the NTWL (170.5 m) with a 44.04% capacity reduction. These integrated elevation–area–capacity (E–A–C) comparisons (Table 4) demonstrate that upper storage bands are disproportionately sensitive to sediment infilling, with shoreline migration and bench expansion driving substantial volumetric penalties (Morris & Fan, 2019). Aligning analyses with standardized control levels ensures consistency with hydrographic documentation (IHO, 2020), while the revised values provide the basis for updating rule curves (Fig. 6) to improve operational reliability.

Table 4 Comparison Of 1982–2025 Area–Elevation–Capacity Values at Control Levels (156–172 m a.m.s.l.)

Elevation (m amsl)	Capacity 1982 (MCM)	Capacity 2025 (MCM)	Loss (MCM)	Area 1982 (km²)	Area 2025 (km²)	Loss (km²)
156	0.00	0.10	−0.10	0.00	0.20	−0.20
160	21.05	8.25	12.80	15.01	6.50	8.51
165	180.06	87.90	92.16	50.99	25.1	25.89
170	564.41	314.10	250.31	101.06	62.5	38.56
NTWL 170.5	614.98	344.15	270.83	106.36	67.02	39.34
172	780.00	400.50	379.50	122.51	74.30	48.21

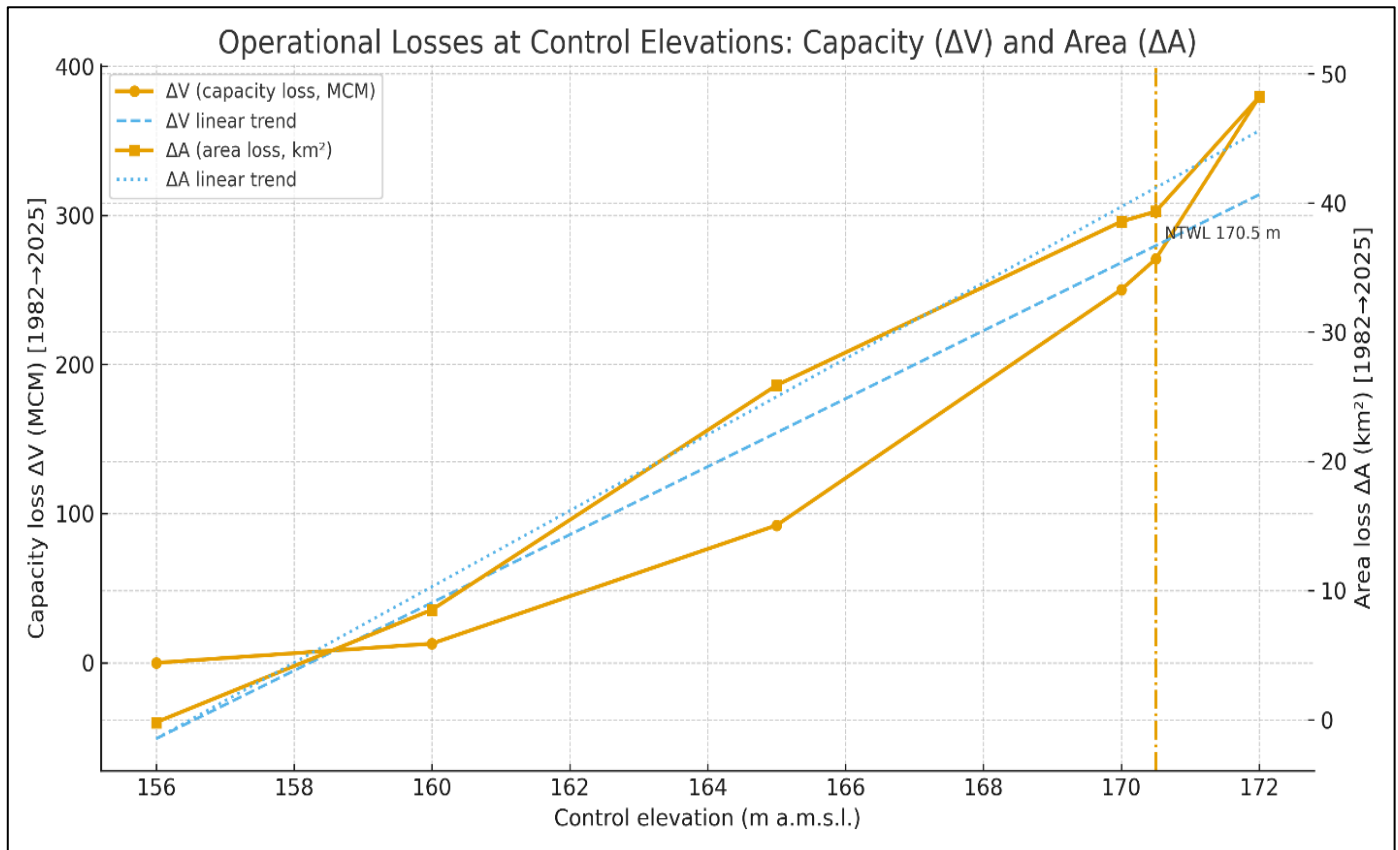Fig 6 Capacity Loss (ΔV, MCM) and Area Loss (ΔA, km²) Versus Control Elevations; NTWL at 170.5 m Indicated.

➢ *Correlation and Change Diagnostics Between Elevation, Area, and Capacity*

Elevation correlates positively with capacity loss (ΔV) and area loss (ΔA), with Pearson's r of 0.60 for ΔV and 0.76 for ΔA, based on band mid-elevations in Table 5. Losses increase by about 7.28 million cubic meters per meter (ΔV) and 1.28 km² (ΔA). ΔV and ΔA strongly correlate with a coefficient of circa 0.97.

Data from regression and Pearson analysis with Fisher z CIS, shown in Figure 7, reveal relationships linked to hypsographic theory, where hydraulic sorting broadens depositional benches and vertical aggradation causes planform and volume penalties. The ΔV- ΔA relationship is partly mechanistic, indicated by *dV/dh=a (h)* and *da/dh=a (h),* focusing on slopes across bands. Effect sizes and uncertainties underscore hydrographic quality control, highlighting elevation's impact on operations. Elevation is a practical control, with bands near thresholds most sensitive, suggesting rule-curve updates and sediment interventions should target specific bands in Table 5.

Table 5 Correlation Input: Mid-Band Elevation vs Capacity/Area Losses (1982 → 2025)

Band (m a.m.s.l.)	Mid-elev (m)	ΔCapacity (MCM)	ΔArea (km²)
151.96–154.23	153.095	−0.05	−0.15
154.23–156.50	155.365	0.1	0.2
156.50–158.77	157.635	2	1.6
158.77–161.04	159.905	6.8	3
161.04–163.32	162.18	15.6	5.1
163.32–165.59	164.455	26.8	6.7
165.59–167.86	166.725	24.3	6.6
167.86–170.13	168.995	−7.30	7
170.13–172.40	171.265	39.2	12.5
172.40–174.67	173.535	270.85	39.34
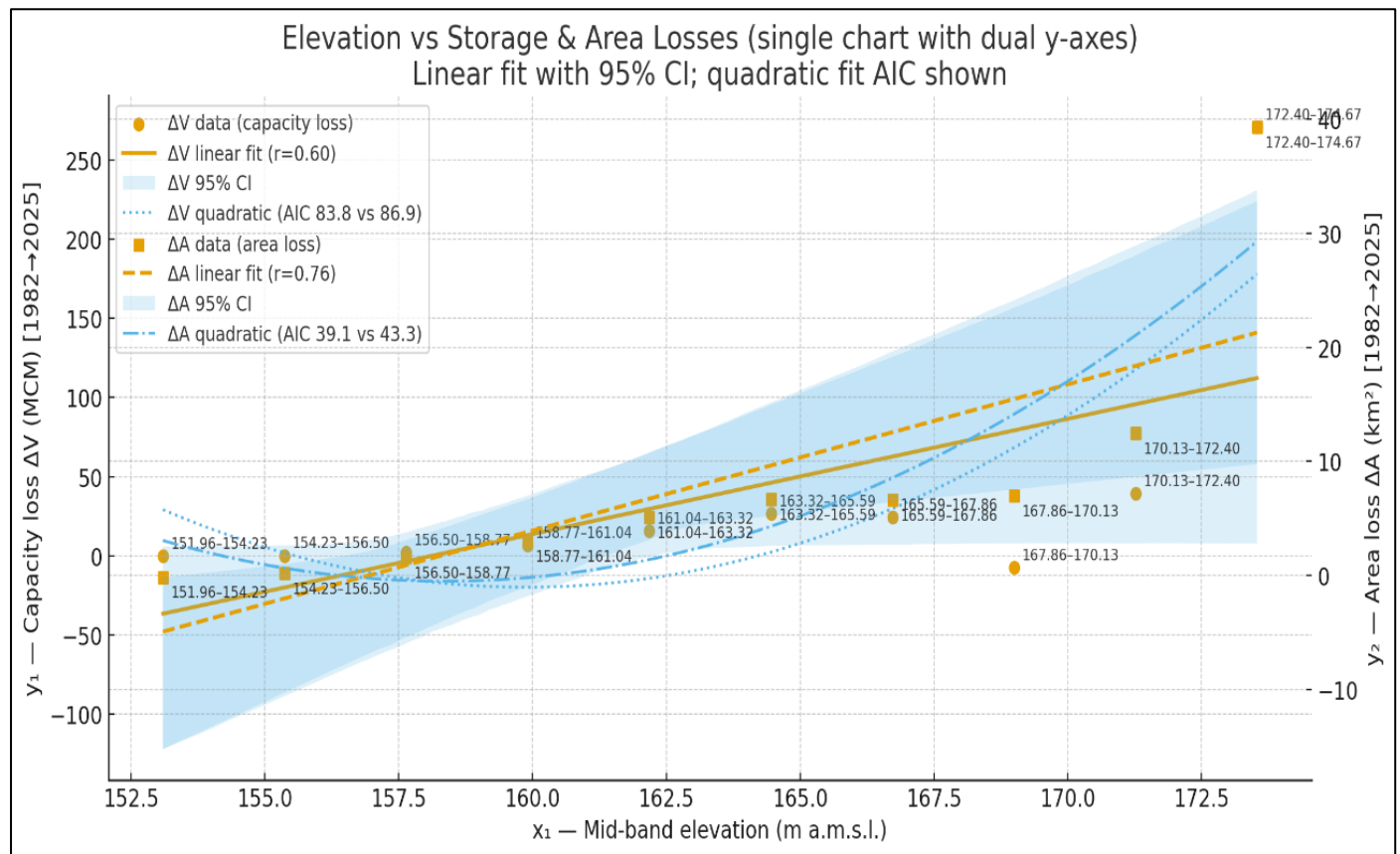
Fig 7 Elevation-Dependent Capacity (ΔV) and Area (ΔA) Losses, Kiri Dam (1982–2025):

Capacity loss ΔV (MCM, left axis) and area loss ΔA (km², right axis) as functions of mid-band elevation (m a.m.s.l.) for Kiri Dam Reservoir. Points are elevation-band midpoints; solid/dashed lines are linear fits with 95% bootstrap CIs; dotted/dash-dot lines show quadratic fits with AIC reported relative to linear.

➤ *PSD–Textural Patterns and Links to Hypsographic Deformation*

Grain-size partitions delineate functional zones: mid-reservoir silty clay (6–52–42%), inflow clay loam (28–35–37%), outflow silty clay loam (13–52–35%), left bank silty clay (9–50–41%), right bank sandy clay loam (60–14–26%); mean Gs = 2.84 ± 0.34 (dimensionless) (Table 3.6; Fig. 3.8a–b). Textures follow USDA classes. Fine, cohesive fractions dominate mid-bench settings (161–167 m), consistent with shoaling and reduced storage efficiency. Bivariate diagnostics show linear trends for silt vs. clay and Gs vs. clay (Fig. 3.8c–d); trend lines are applied only to continuous variables, and error bars are omitted because $n = 1$ per site. Collectively, PSD and density patterns corroborate hypsographic vulnerability of the mid-bench and justify elevation-focused maintenance.

Table 6 Particle Size Distribution and Textural Classification

| Sampling Location	Coordinates (Lat, Long)	Spec. Gravity (Gs)	Sand (%)	Silt (%)	Clay (%)	Textural Class
Inflow	7°25′18″N, 3°51′12″E	2.34	28	35	37	Clay loam
Mid Reservoir	7°25′28″N, 3°51′25″E	3.12	6	52	42	Silty clay
Outflow	7°25′26″N, 3°51′39″E	2.92	13	52	35	Silty clay loam
Left Bank	7°25′22″N, 3°51′33″E	2.67	9	50	41	Silty clay
Right Bank	7°25′28″N, 3°51′34″E	3.17	60	14	26	Sandy clay loam
Mean ± SD		2.84 ± 0.34	23.2 ± 22.4	40.6 ± 15.8	36.2 ± 6.8	
Min–Max		2.34	6	14	26	
Max		3.17	60	52	42	
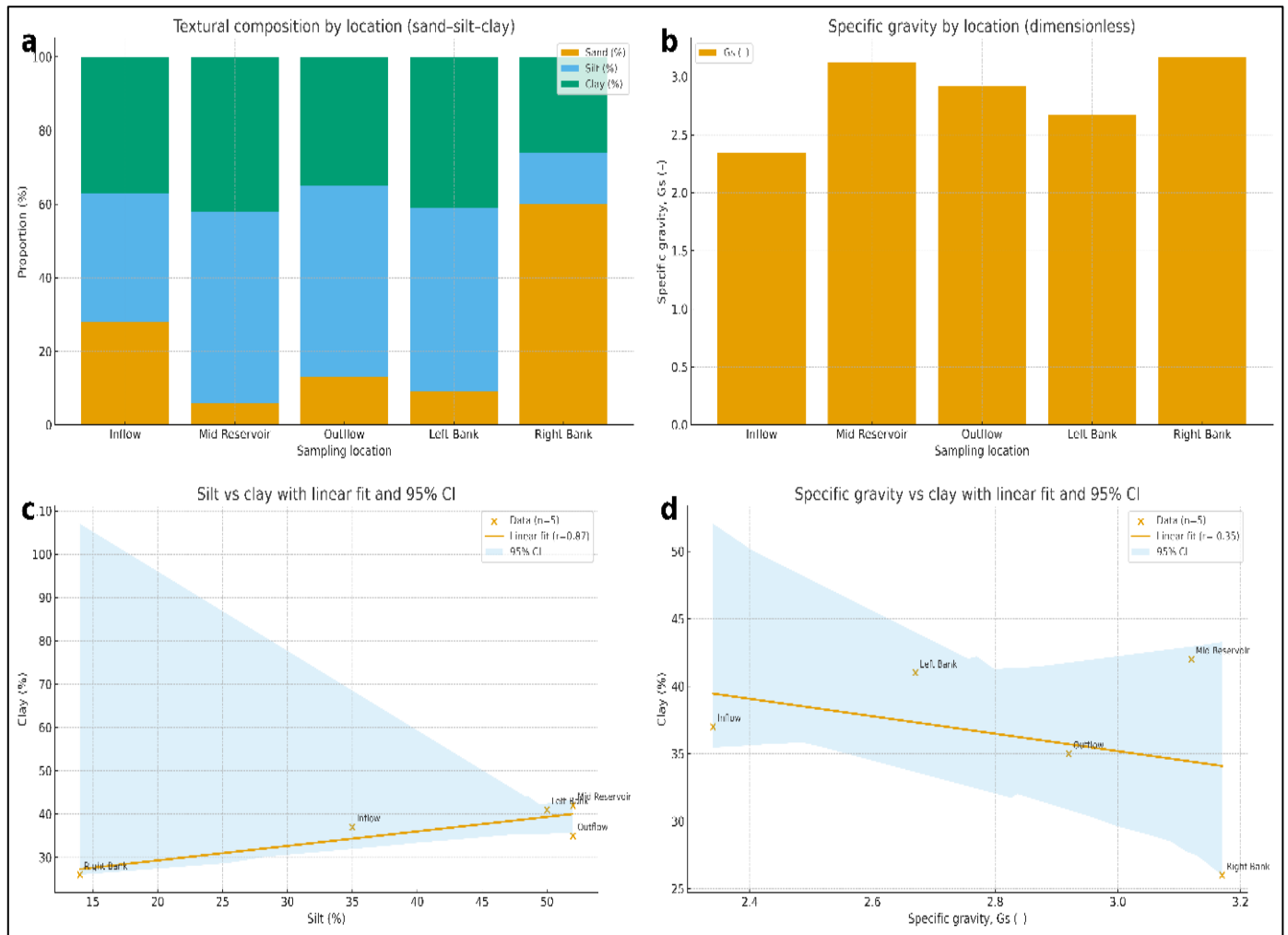
Fig 8 A-D. Sediment Texture and Density Diagnostics by Location.

Panels: a) sand–silt–clay composition (stacked, %); b) specific gravity Gs; c) silt vs. clay with linear fit and 95% bootstrap CI; d) Gs vs. clay with linear fit and 95% bootstrap CI.

➤ *Geochemical Signatures and Management Relevance*

Geochemistry (Fig. 3.9a–e; Table 6). The pH levels are near-neutral, from 6.94 to 7.39 (Fig. 9 a). Highest TOC and TN are at the outflow (TOC 1.71%, TN 0.142%) and left bank (TOC 1.69%, TN 0.135%), with moderate levels at the mid-reservoir (TOC 1.32%, TN 0.106%) and lowest on the sandy right bank (TOC 0.83%, TN 0.075%) (Fig. 9 b). This suggests effective trapping of fines and organic matter. Moderate available phosphorus (10.2-15.9 mg kg⁻¹) peaks at outflow and left bank (Fig. 9 c). Metal levels are moderate: Pb (16-26 mg kg⁻¹), Cu (12-19 mg kg⁻¹), Zn (63-71 mg kg⁻¹), near-zero on the right bank, possibly due to coarse sediment with low binding capacity (Fig. 9 d). ΣPAHs and ΣPCBs are low, highest at outflow, nearly zero on the right bank (Fig. 9 e). The mid-bench (161–167 m) and outflow are hotspots for fine fractions. Sentinel parameters—TOC, TN, Av-P, and metals—should be prioritised there, with the right bank as a coarse-control site.

Table 7 Surface-Sediment Geochemistry by Location, Kiri Dam (2025).

| Location	Coordinates (DMS)	pH	TOC (%)	TN (%)	Av-P (mg kg⁻¹)	Pb (mg kg⁻¹)	Cu (mg kg⁻¹)	Zn (mg kg⁻¹)	ΣPAHs (mg kg⁻¹)	ΣPCBs (mg kg⁻¹)
Inflow	7°25′18″N, 3°51′12″E	7.27	1.52	0.127	14.8	23	17	63	0.654	0.0301
Mid Reservoir	7°25′28″N, 3°51′25″E	7.27	1.32	0.106	12.2	24	17	65	0.533	0.0244
Outflow	7°25′26″N, 3°51′39″E	7.38	1.71	0.142	15.9	26	19	70	0.775	0.0373
Left Bank	7°25′22″N, 3°51′33″E	7.39	1.69	0.135	15.2	26	19	71	0.764	0.0369
Right Bank	7°25′28″N, 3°51′34″E	6.94	0.83	0.075	10.2	16	12	0	0	0
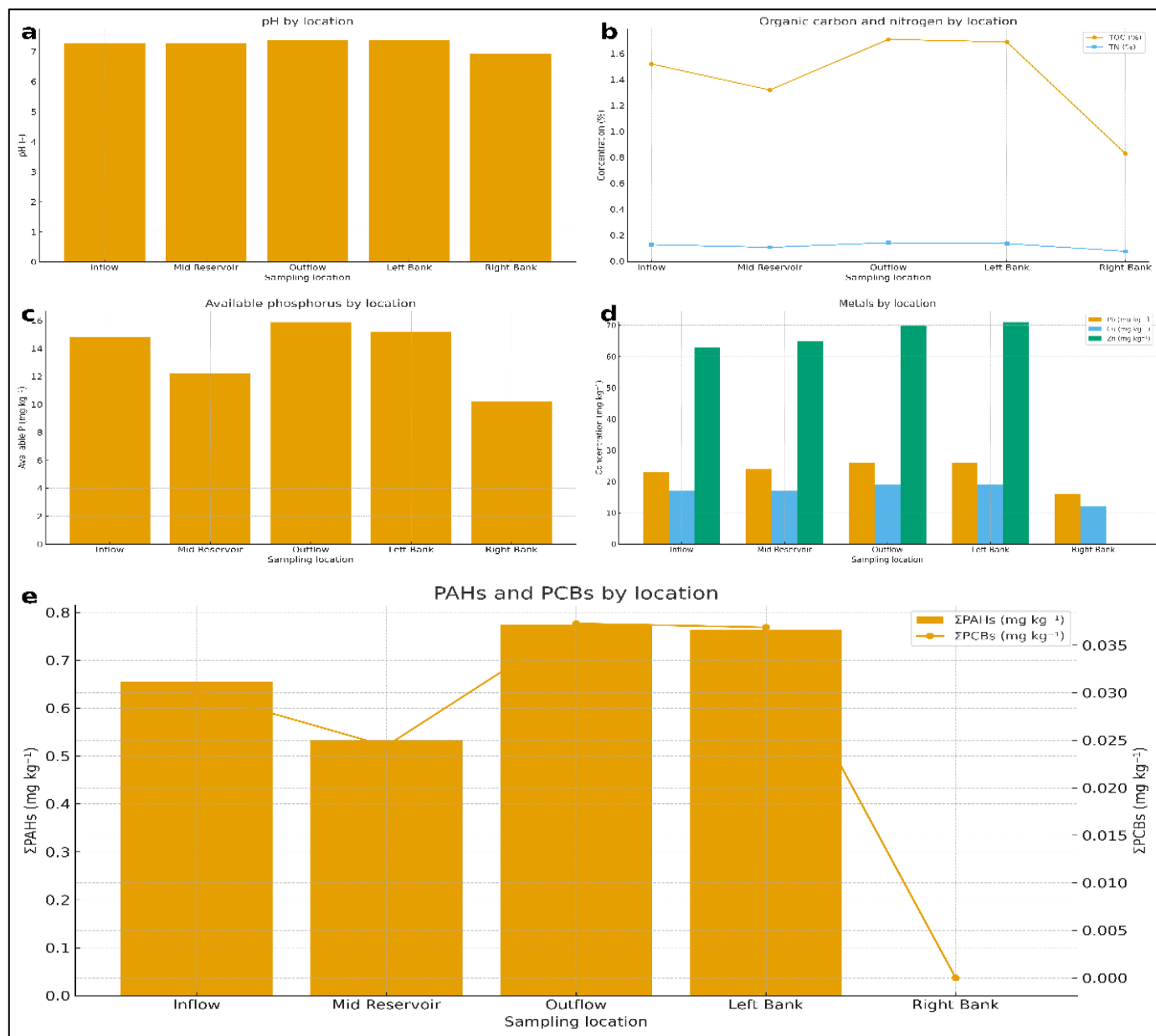
Fig 9 A-E. Spatial Variation of Sediment Geochemistry by Location in Kiri Dam (2025).

Panels: a) pH by location; b) TOC & TN by location; c) Available phosphorus by location; d) Metals (Pb, Cu, Zn) by location; and e) ΣPAHs (bars, left y-axis) and ΣPCBs.

> *Summary of Capacity/Area Change*

Between 1982 and 2025, storage decreased by 270.83 million cubic meters (−44.04%) and water spread by 39.34 square kilometres (−37.0%) (see Table 7). The volume–area loss elasticity is 1.19, indicating capacity contracted disproportionately relative to the planform geometry,

consistent with hypsographic compression on extensive benches. Capacity loss per unit area is about 6.89 million cubic meters per square kilometres. In comparison, the basin-wide depth-weighted capacity density declined from approximately 5.78 to 5.14 million cubic meters per square kilometres (about 11%), reflecting basin-wide shallowing. Figure 10 shows this imbalance—a steeper decline in capacity than area—supporting the idea of vertical aggradation rather than shoreline retreat.

Table 8 Capacity and Surface Area Decline (1982–2025)

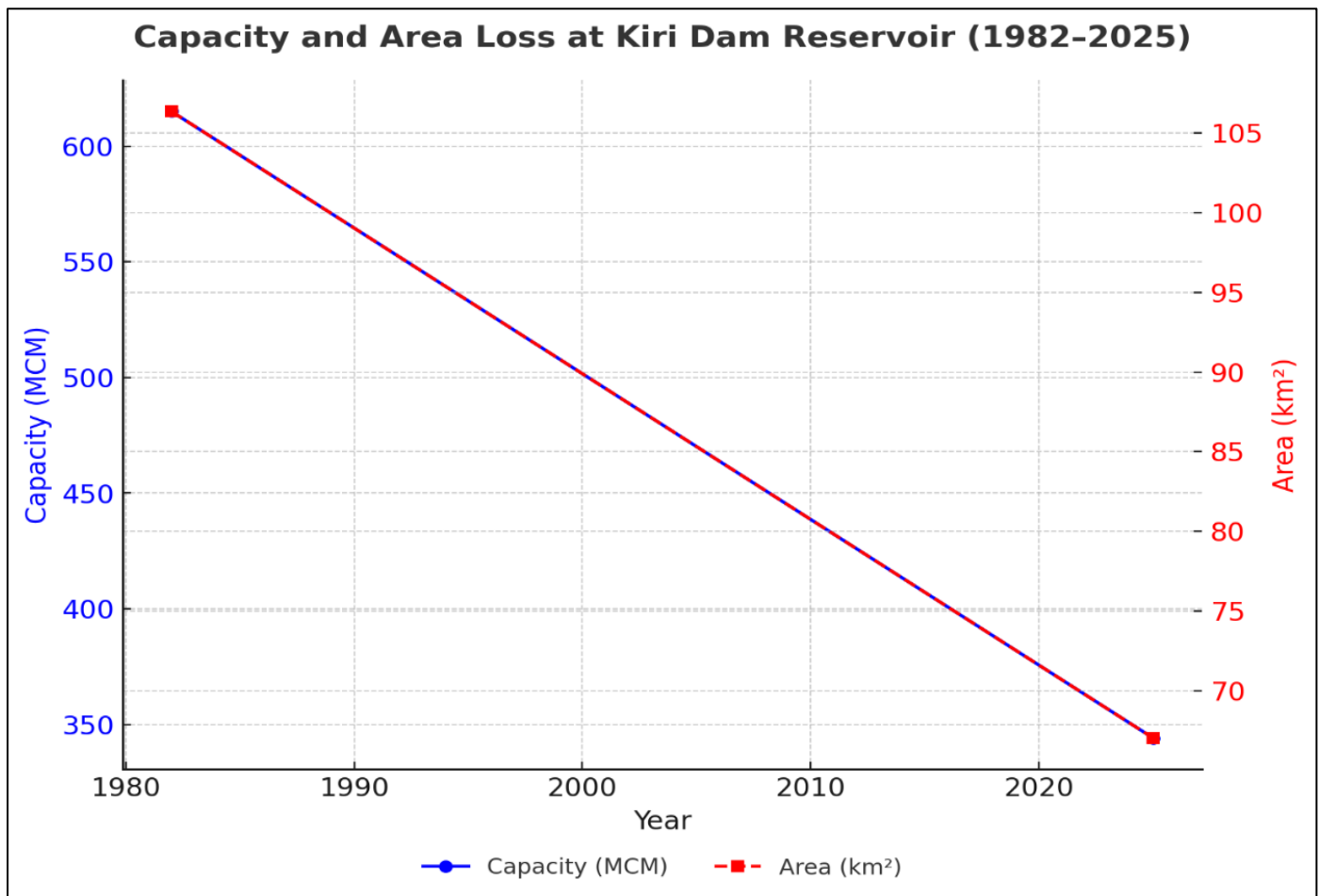| Year / Epoch	Capacity (MCM)	Surface Area (km²)	Capacity Loss (MCM)	% Capacity Loss	Area Loss (km²)	% Area Loss
1982 (Design)	615.00	106.36	0.00	0.00	0.00	0.00
2025 (Survey)	344.15	67.02	270.83	44.04	39.34	37.00

Fig 10 Capacity vs Surface Area Decline (1982–2025)

> *Synthesis of Findings*

Evidence from E–A–C update, banding, particle-size, and geochemical analyses shows elevation-banded sedimentation reducing live storage. Losses are focused on 161–167 m mid-reservoir benches, making up over 60% of decline below 167 m. A strong linear correlation (r^2 ~0.99) between elevation and capacity/area confirms coherent hypsographic profiles despite infill. At NTWL of 170.5 m, storage volume and surface area are about 44% and 37% below original specs. Silty-clay textures and geochemical signatures like TOC, TN, Av-P, and trace metals support observed shoaling and water redistribution.

> *Operational Implications for Kiri Dam*

Rule curves should be re-parameterized with the 2025 E–A–C to prevent over-estimation near NTWL. Prioritize bench-focused dredging and delta-front management in the 161–167 m bands for maximum capacity gain. Maintain a seasonal flood buffer proportional to reduced live storage; coordinate drawdowns for sediment evacuation. Focus on mid-bench and shallow plains (>170 m) for nutrient and metal monitoring, aligning with habitats in Tables 5 and 6.

Implement catchment measures like bank stabilisation, gully checks, and land-use practices to reduce sediment runoff.

> *Monitoring Framework and Research Needs (with Conceptual Framework)*

To implement the evidence, we create a feedback loop linking catchment drivers with hypsographic changes and management decisions. The framework includes: (i) drivers like rainfall seasonality and land use; (ii) reservoir hydraulics such as circulation; (iii) depositional zones at mid-bench (161–167 m) and delta front (>170 m); (iv) measurements using GNSS/RTK, ADCP, CTD, with quality checks; (v) diagnostics involving TIN-to-raster, E–A–C calculations, and geochemical analyses; (vi) hypsographic deformation risking live-storage loss near NTWL, flood buffers, and water quality; (vii) interventions like rule-curve updates, dredging, delta management, and catchment controls; and (viii) monitoring through resurveys, shoreline tracking, recovery of MCM, and trend analysis. Feedback directs measurements and interventions to vulnerable elevation zones (161–167 m). See Figure 11.
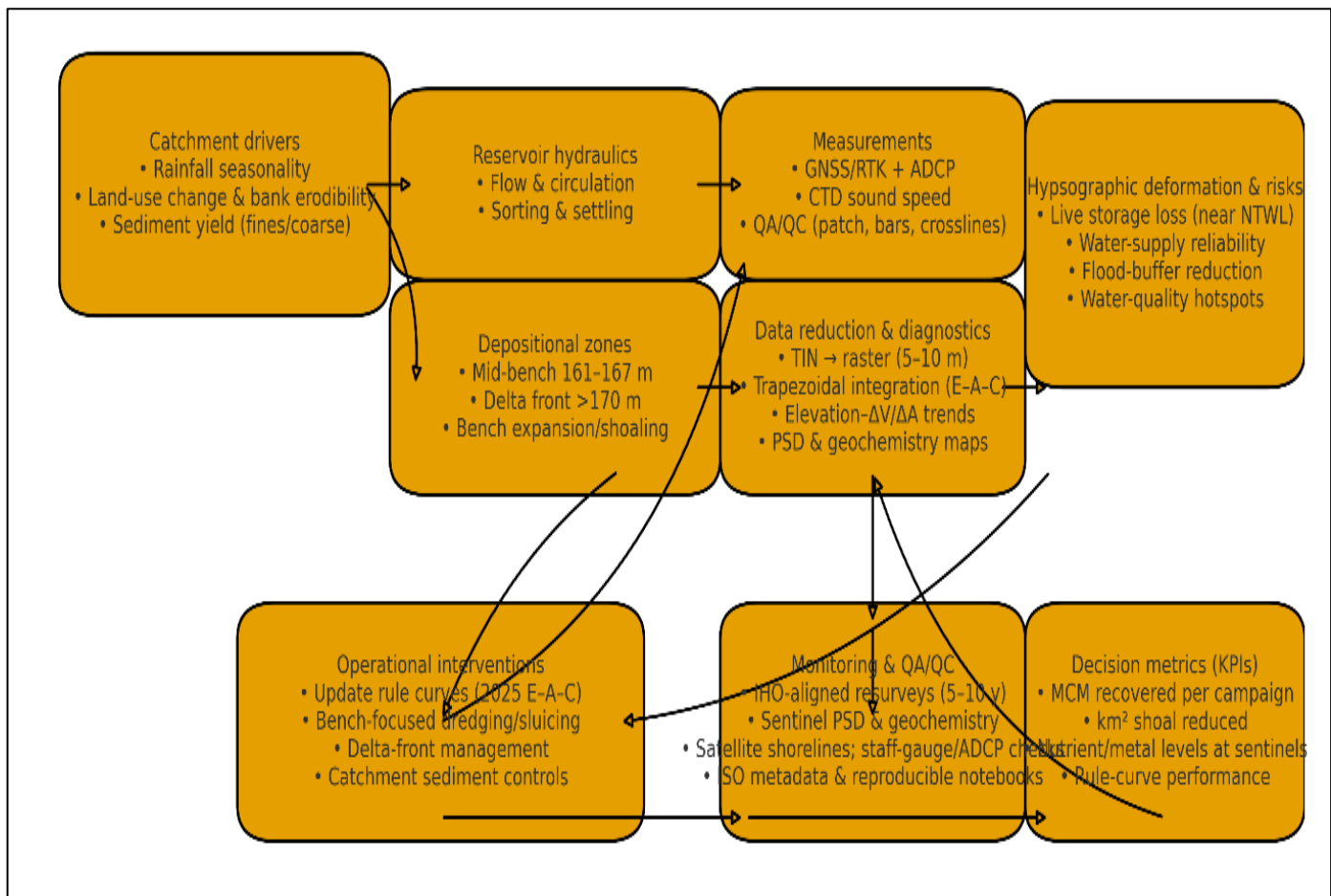
Fig 11 Conceptual Framework Linking Sediment Drivers, Hypsographic Change, and Management Responses.

IV. CONCLUSIONS AND RECOMMENDATIONS

➢ *Principal Conclusions*

A comparison of 1982 and 2025 shows a systematic sedimentation pattern causing reduced capacity at Kiri Dam. At NTWL 170.5 m, storage and water spread decreased by 44.04% (−270.83 million m³) and 37% (−39.34 km²). Most losses are in the 161–167 m mid-bench zone, increasing the elevation–capacity gradient. A strong linear link (r² 0.99) between elevation and capacity/area highlights a coherent hypsography. PSD and geochemical tests confirm fine sediment dominance and moderate nutrient/metal retention, posing localized water quality risks but no acute contamination. The evidence-operations link is summarized in Figure 11.

➢ *Actionable Recommendations*

• *Rule-Curve Updates (use 2025 E–A–C)*

✓ Re-parameterize operating rule curves with the 2025 elevation–area–capacity dataset to remove over-estimation near NTWL.
✓ Embed uncertainty bands from hydrographic QC (e.g., crossline residuals ≤0.12 m; horizontal/vertical RMSE ≤0.03/0.05 m) to guide conservative allocations and flood routing.

✓ Recompute seasonal yield/flood set-points for current geometry; apply band-aware guidance when the pool resides within 161–167 m.
✓ *4.2.2 Bench-targeted sediment management (161–167 m priority)*
✓ Focus on mechanical dredging (amphibious/dry windows) and/or hydraulic sluicing/flushing on mid-bench cells; coordinate with controlled drawdowns to maximise export.
✓ Sequence works forebay → delta front to avoid re-deposition; deploy temporary silt curtains where feasible.
✓ Implement compliant spoil handling (dewatering, beneficial reuse, or licensed disposal).
✓ Track outcomes with KPIs (below).
✓ *4.2.3 Catchment sediment controls (source reduction)*
✓ Stabilize banks/gullies in priority tributaries; install grade-control/check structures; restore riparian buffers.
✓ Improve road/farm drainage (cross-drains, dissipation basins, sediment traps) to cut storm-driven fines.
✓ Promote soil-cover practices (cover crops, residue retention).
✓ Verify effectiveness with tributary turbidity/TSS targets and shoreline-change metrics from satellite imagery.

• *Monitoring Cadence and QA (IHO-Aligned)*

✓ Institutionalise resurveys every 5–10 years (shorter after extreme floods) following IHO S-44 quality

recommendations: RTK/DGPS control, sound-speed profiles, patch tests, daily bar checks, ≥10% crosslines, and documented uncertainty budgets.
- ✓ Maintain reproducibility by archiving RINEX/sonar/CTD logs, QA reports, TINs/rasters, and notebooks, and by regenerating figures/tables from the archive.
- ✓ Operate sentinel stations (PSD, geochemistry) at mid-bench and delta-front sites each wet/dry season.

➤ *SMART Performance Targets (KPIs)*

- Capacity recovery: ≥15–25 MCM recovered in 3 years within 161–167 m bands (post-campaign E–A–C re-integration).

- Flood buffer: Maintain ≥X MCM live-storage margin by 1 May annually (value X set from updated rule-curves and risk tolerance).
- Sediment reduction: ≥20–30% reduction in median wet-season TSS at priority tributary mouths within 2 years of catchment works.
- Water quality: No upward trend in mid-bench Av-P and trace metals over 3 years at sentinel sites (non-parametric trend test).
- Survey quality: Crossline median absolute vertical residuals ≤0.12 m; horizontal/vertical RMSE ≤0.03/0.05 m per campaign.

Table 9 Prioritization and Feasibility (Risk–Cost View)

Action (focus)	Expected impact	Cost/complexity	Key dependencies
Bench dredging/sluicing (161–167 m)	High (direct MCM gain)	Moderate–High	Drawdown windows; disposal/reuse plan
Delta-front management (>170 m)	Medium–High	Moderate	Flow windows; curtain logistics
Catchment controls (priority tributaries)	Medium (sustained)	Moderate	Landholder buy-in; design/permits
Rule-curve update (2025 E–A–C)	High (system-wide)	Low	Governance review; modeling support
Sentinel monitoring (PSD/chem; shoreline)	Medium (early warning)	Low	Lab capacity; EO analytics

➤ *Governance and Operationalization*

- Lead operator: Upper Benue River Basin Development Authority (UBRBDA), with irrigation stakeholders.
- Windows: Schedule dry-season drawdowns (lowest ecological sensitivity) for dredging/sluicing; align sluice releases with moderate inflows to enhance export without downstream risk.
- Decision process: Annual review of KPIs and updated E–A–C; adaptive adjustment of rule-curves and work plans via the feedback loop in Figure 10.

➤ *Limitations and Future Work*

- Temporal scope: Geochemistry/PSD reflect single-season sampling at n=5 locations; results show patterns, not full seasonal data envelopes.
- Spatial sampling: Interpolation causes uncertainty in sparsely sampled or hazard-limited areas; uncertainty budgets are provided, but small-scale heterogeneity may remain.
- This study infers mechanisms from morphology and textures; targeted sediment-transport monitoring would refine parameterization. Future work should (i) expand sentinel networks, (ii) benchmark hydrodynamic–sediment models under updated geometry, and (iii) evaluate nature-based delta-front stabilization options alongside mechanical measures.

➤ *Closing Remark*

This study offers a reproducible, standards-aligned reassessment of Kiri Dam, using two-epoch bathymetry, hypsographic diagnostics, and sediment texturing within a practical management framework. The model converts evidence into rule-curve updates, sediment management, catchment controls, and IHO monitoring. This workflow is adaptable to Sudano–Sahel reservoirs where fine sediments reduce storage at operational levels. When used adaptively, these measures can boost capacity, preserve flood buffers, and lower water-quality risks. Future research should include morphodynamics with hydro-sediment modelling and perform cost–benefit analyses.

- *Author Contributions (CRediT)*

- ✓ Conceptualization: A.T. Gambo, O.S. Olaniyan;
- ✓ Methodology: A.T. Gambo, A.A. Adegbola;
- ✓ Investigation: A.T. Gambo;
- ✓ Formal analysis: A.T. Gambo, O.S. Olaniyan;
- ✓ Writing – original draft: A.T. Gambo;
- ✓ Writing – review & editing: O.S. Olaniyan, A.A. Adegbola;
- ✓ Supervision: O.S. Olaniyan.

➤ *Conflicts of Interest*

The authors declare no conflicts of interest, financial or personal, that could have influenced.

➢ *Data Availability*

The datasets are available upon request from the corresponding author.

REFERENCES

[1]. American Public Health Association (APHA), American Water Works Association (AWWA) and Water Environment Federation (WEF), 2017. *Standard methods for the examination of water and wastewater*. 23rd ed. Washington, DC: APHA.

[2]. Domínguez-Gálvez, D.L. and Álvarez-Álvarez, M.J., 2025. Sustainable sediment management in reservoirs: La Estancilla case study. *Journal of Water and Land Development*, 64, pp.211–220.

[3]. International Hydrographic Organisation (IHO), 2020. *S-44: Standards for Hydrographic Surveys*. Ed. 6.0.0. Monaco: IHO.

[4]. International Hydrographic Organisation (IHO), 2022. *S-44: Standards for Hydrographic Surveys*. Ed. 6.1.0. Monaco: IHO.

[5]. Kondolf, G.M., Rubin, Z.K. and Minear, J.T., 2014. Sustainable sediment management in reservoirs and regulated rivers. *Earth Surface Processes and Landforms*, 39, pp.18–37.

[6]. Li, J., Zhang, C. and Wu, P., 2020. Reservoir sedimentation and water-supply risk in semi-arid basins. *Water Resources Research*, 56, e2020WR027517.

[7]. Morris, G.L. and Fan, J., 1998. *Reservoir sedimentation handbook*. New York: McGraw-Hill.

[8]. Punuf, D.A., Sartohadi, J. and Setiawan, M.A., 2025. Community-based management of small reservoirs in areas prone to erosion, landslides, and drought. *Environmental Sustainability*, 15(1), pp.83–96.

[9]. United States Army Corps of Engineers (USACE), 2013. *EM 1110-2-1003: Hydrographic surveying*. Washington, DC: USACE.

[10]. United States Bureau of Reclamation (USBR), 1985. *Area-capacity curves for reservoirs*. Denver, CO: USBR.